Quantitative proteomic and transcriptional analyses reveal degradation pathway of γ-hexachlorocyclohexane and the metabolic context in the actinobacterium *Streptomyces* sp. M7

Pedro E. Sineli [a], Hector M. Herrera [a], Sergio A. Cuozzo [a, b], José S. Dávila Costa [a, *]

[a] *Planta Piloto de Procesos Industriales Microbiológicos (PROIMI-CONICET), Tucumán, Argentina*
[b] *Facultad de Ciencias Naturales e Instituto Miguel Lillo, Universidad Nacional de Tucumán, Tucumán, Argentina*

HIGHLIGHTS

- Lindane degradation in *Streptomyces* sp. M7 occurs via up- and down-stream pathways.
- Unusual enzymes participate in the down-stream pathway.
- Degradation is supported by an active catabolism that supplies energy and NADPH.
- Complete lindane degradation in actinobacteria is proposed for the first time.

GRAPHICAL ABSTRACT
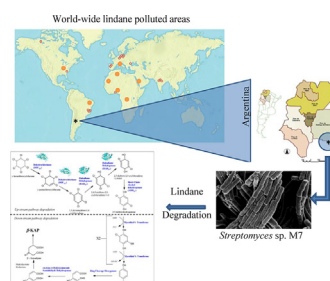
ARTICLE INFO

ABSTRACT

Highly contaminated γ-hexachlorocyclohexane (lindane) areas were reported worldwide. Low aqueous solubility and high hydrophobicity make lindane particularly resistant to microbial degradation. Physiological and genetic *Streptomyces* features make this genus more appropriate for bioremediation compared with others. Complete degradation of lindane was only proposed in the genus *Sphingobium* although the metabolic context of the degradation was not considered. *Streptomyces* sp.M7 has demonstrated ability to remove lindane from culture media and soils. In this study, we used MS-based label-free quantitative proteomic, RT-qPCR and exhaustive bioinformatic analysis to understand lindane degradation and its metabolic context in *Streptomyces* sp. M7. We identified the proteins involved in the up-stream degradation pathway. In addition, results demonstrated that mineralization of lindane is feasible since proteins from an unusual down-stream degradation pathway were also identified. Degradative steps were supported by an active catabolism that supplied energy and reducing equivalents in the form of NADPH. To our knowledge, this is the first study in which degradation steps of an organochlorine compound and metabolic context are elucidate in a biotechnological genus as *Streptomyces*. These results serve as basement to study other degradative actinobacteria and to improve the degradation processes of *Streptomyces* sp. M7.

© 2018 Elsevier Ltd. All rights reserved.

* Corresponding author. Planta Piloto de Procesos Industriales Microbiológicos (PROIMI-CONICET), Av. Belgrano y Pje. Caseros, San Miguel de Tucumán-Argentina, CP 4000, Argentina. .
E-mail addresses: jsdavilacosta@gmail.com, jsdavila@proimi.org.ar (J.S. Dávila Costa).

1. Introduction

Scarcity of agricultural land and the increasing demand of food encouraged the use of pesticides to improve the yield of crops.

1,2,3,4,5,6-hexachlorocyclohexane (HCH) is a chlorinated pesticide used to protect crops from vector borne diseases. HCH was classified as a dangerous organic contaminant due to its persistence in the environment and acute toxicity (Bindra et al., 2010). Highly contaminated areas with HCH were reported in Japan, Canada, South Africa, India, Argentina, Germany, Eastern Europe, Greece and United States (Lal et al., 2010). HCH exists as a mixture of eight isomers known as technical lindane. The gamma isomer (γ-HCH or lindane) is the active component used as insecticide. Uncontrolled application and inappropriate handling of lindane led to contamination of soils, biota and waters (Miglioranza et al., 2013; Vijgen et al., 2011). The low aqueous solubility and high hydrophobicity make lindane particularly resistant to microbial degradation. Actinobacteria is a diverse phylum characterized by its metabolic versatility (Goodfellow, 2012). Within actinobacteria, genus *Streptomyces* is recognized by its biotechnological potential. Physiological and genetic features of this genus make it more appropriate for bioremediation processes compared with other bacteria (Alvarez et al., 2017). *Streptomyces* sp. M7, isolated from a highly polluted area, is able to remove lindane from liquid culture media and different kind of soils (Aparicio et al., 2015; Simon Sola et al., 2017). Degradation pathway used by this strain was not elucidated. Complete degradation pathway of lindane was only proposed in the genus *Sphingobium* (Nagata et al., 1999) although its metabolic context was never considered.

The aerobic biodegradation of lindane encompasses two pathways, the up and down-stream degradation pathways. Several studies have demonstrated that steps from the up-stream are crucial for the degradation (Nagata et al., 1999, 2001; 2007). Enzymes encoded by the genes *linA*, *linB* and *linC*, which compose the up-stream pathway, are the responsible for initial dechlorination of the lindane molecule. LinA is believe to be a unique type of dehydrochlorinase and might present several variants according to the microorganism. LinB is a haloalkane dehalogenase while LinC, the less studied enzyme of the up-stream pathway, presents dehydrogenase activity (Lal et al., 2010). The down-stream pathway may be considered more complex in terms of number and variants of enzymes. Several genes have been linked to this pathway, among them *linD,E,F,G,H,J* (Lal et al., 2010). The genes *linD* and *lindE* encodes the reductive dechlorinase and ring cleavage oxygenase, respectively. Besides, these genes might be considered the most important since degradation of lindane may be completed via β-ketoadipate pathway (Wells and Ragauskas, 2012).

In the present work, we used MS-based label-free quantitative proteomic, Real time PCR and exhaustive bioinformatic analysis to elucidate lindane degradation steps and understand its metabolic context in *Streptomyces* sp. M7. Comparing cells grown in the presence of lindane to untreated cells, we identified the proteins involved in the up-stream degradation pathway. In addition, our study showed that mineralization of lindane is feasible since proteins of the down-stream degradation pathway were also identified.

To our knowledge, this is the first study in which proteomic and transcriptional approaches are used to elucidate degradation mechanisms of organochlorine compounds in a biotechnological genus as *Streptomyces*. Understanding lindane degradation and its metabolic context in *Streptomyces* sp. M7 will help to improve the global process and serve as model to study other actinobacteria with biotechnological potential.

2. Materials and methods

2.1. Strain, culture medium, growth conditions

Streptomyces sp. M7 isolated from polluted sediments (Benimeli et al., 2003) was incubated at 30 °C and 150 r.p.m. in TSB medium during 48 h to promote cellular growth. Afterwards, cells were harvested, washed and split (0.1 mg ml^{-1} of cells) into two minimal medium (MM) subcultures. MM is composed of (g L^{-1}): NH$_4$SO$_4$, 4; K$_2$HPO$_4$, 0.5; MgSO$_4$·7H$_2$O, 0.2; FeSO$_4$·7H$_2$O, 0.01 and pH 7. One subculture was supplemented with lindane 5 mg L^{-1} (MM$_L$) while glucose 1 g L^{-1} was used as carbon source in the remaining subculture (MM$_G$). Cells were incubated under the same conditions during 120 h and residual lindane was determined every 24 h. Biomass was estimated by washing the pellets with 25 mM Tris–EDTA buffer (pH 8.0) and drying to constant weight at 105 °C.

2.2. Determination of residual lindane

Residual lindane in cell-free supernatants was extracted by solid-phase extraction using a C18 column (Varian, Lake Forest, USA). Lindane concentration was quantified in a Gas Chromatograph (Agilent 7890A) equipped with ^{63}Ni micro-Electron Capture Detector (GC-μECD), HP5 capillary column (30 m × 0.53 mm × 0.35 m), a split/splitless Agilent 7693 B injector and Agilent ChemStation software. The chromatographic conditions were as follows: carrier gas (nitrogen) flow rate: 25 cm s^{-1}, initial oven temperature: 90 °C increasing to 180 °C at 30 °C min^{-1}, and increasing to 290 °C at 20 °C min^{-1}, detector temperature: 320 °C and injection volume: 1 mL. Quantitative sample analysis was performed using a calibration curve with appropriated dilutions of lindane calibration standards (AccuStandard, New Haven, USA).

2.3. Protein extracts for label-free quantitative proteomic analysis

Cells grown in MM$_L$ and MM$_G$ (control) were harvested in logarithmic phase of growth. Protein extracts were prepared according to the methodology previously described by Dávila Costa et al. (2015). Briefly, cells were washed with washing buffer (25 mM Tris buffer pH 7, 2 mM EDTA), resuspended in the same buffer and crushed with liquid nitrogen. Protein integrity was determined by SDS-PAGE and the concentration was measured by Bradford. 50 μg of proteins were treated with 20 μl of reducing solution (200 mM DTT, 100 mM Tris, pH 7.8) and alkylation solution (200 mM iodoacetamide, 100 mM Tris, pH 7.8). Samples were incubated 1 h at RT with each solution and proteins were then precipitated with TCA 10%. After centrifugation (16,100 g, 30 min, 4 °C), protein pellet was washed three times by rinsing with pre-chilled (−20 °C) acetone. Protein pellet was then resuspended with 50 mM ammonium bicarbonate up to a concentration of 10 μg μl^{-1} and 50 μg of proteins were digested with trypsin. Finally, digested proteins were purified with a Zip-Tip C18 column stored at −80 °C until subjected to MS analysis.

2.4. LC-MS/MS analysis of protein extracts

LC-MS/MS experiments were carried out from at least three biologically independent replicates. Samples were dissolved in trifluoroacetic acid and LC of the peptide samples were performed using a Thermo Scientific-EASY-nLC 1000 equipped with an Easy-Spray Column PepMap RSLC (C18, 2 μm, 100A, 50 μm × 150 mm). A gradient with two solutions was used (Solution A, 0.1% formic acid (v/v); Solution B, acetonitrile with 0.1% formic acid). Peptides were eluted with a gradient of 7% B to 95% B over 135 min at flow rate of 0.300 μl min^{-1}. Mass spectra were obtained by a Q-Exactive Orbitrap instrument (Thermo Fisher Scientific). Instrument configuration allowed the identification of peptides to be carried out at the same time that they were separated by chromatography, obtaining Full MS and MS/MS. The 20 most intense peaks in each

MS spectrum were selected for MS/MS fragmentation. LC-MS/MS of protein extract was performed in CEQUIBIEM-University of Buenos Aires-Argentina.

2.5. Data analysis − protein quantification

Data analysis was performed using the softwares Proteome Discoverer 2.1 and Perseus. Samples obtained from MM_L were compared to the corresponding MM_G samples. Protein database of *Streptomyces* sp. M7 was used for peptide identification. Proteins were considered significantly regulated when: (1) they showed on average an increase '2-fold in their abundance; (2) *t*-test showed a ρ-value below 0.05. ρ-value and statistical parameters were calculated by Perseus software. To estimate the limit of detection of our instrument on the protein level, we considered the ninety-ninth percentile of the area of all proteins identified by Proteome Discoverer passing the identification score threshold with a false discovery rate of 0.01. This value was 590898. We then used this value to impute missing area values in our label-free quantitation. Area values were expressed as $\log_2$.

2.6. Quantitative Real-time PCR (RT-qPCR)

Cells grown up to logarithmic phase of growth in MM_L and MM_G (control) were used to extract total RNA. Cells were washed, resuspended in RNAprotect Bacteria Reagent (Quiagen) and crushed with liquid nitrogen. Total RNAs of *Streptomyces* sp. M7 were obtained according to SV RNA Isolation System Kit (Promega). Genomic DNA was removed by incubating one unit of RQ1 RNase-Free DNase (Promega) per 1 μg of RNA for 30 min at 37 °C. Complete elimination of DNA was evaluated by PCR. RNA concentration was calculated by determining the absorbance at 260 nm. Quality of RNA was assessed by measuring A260/280 and A260/230 ratios as well as by electrophoresis in a formaldehyde denaturing agarose gel.

The cDNAs for RT-qPCR were synthesized from 1 μg of RNA by using ImProm-II Reverse Transcriptase reagent kit (Promega). RT-qPCR was performed using Power SYBR Green PCR Master Mix on StepOnePlus Real-Time PCR system (Applied Biosystem). Cycling parameters of reactions consisted of an initial step of 10 min at 95 °C followed by 40 cycles of denaturation at 95 °C for 15 s, annealing/extension at 60 °C for 60 s. Relative quantification of genes was analyzed with the $2^{-\Delta\Delta Ct}$ method. The expression of *hrdA* (present in the genome at a single copy), thought to encode a RNA polymerase sigma factor, was monitored and validated to normalize the relative transcription of analyzed genes. Technical triplicates of RT-qPCR were carried out for each biological replicate and quantification was performed according to the average values. Melting curve and primers efficiency were evaluated using StepOne software 2.3 (Applied Biosystem). Primers and PCR products are listed in Table S1.

2.7. Homology models

Models for enzymes of the up-stream degradation pathway of lindane were constructed using the homology modelling approach as implemented in the program Modeller v9.14 by Phyton software. Template crystal structures, obtained from PDB data bank (RCSB-PDB), were 3A76 for dehydrochlorinase, 4HZG for haloalkane dehalogenase and 4WEC for short-chain alcohol dehydrogenase. Protein structures were visualized using PyMol. DOPE profile graphics were generated to compare similarity between the model and the template. Models quality was evaluated by analyzing their stereochemical accuracy and their folding reliability. Thus, Ramachandran analysis for each model was generated using MolProbity

server (Chen et al., 2010). Z-score was determined through ProSA server (Wiederstein and Sippl, 2007).

2.8. Data availability

Whole Genome Shotgun project has been deposited at DDBJ/ENA/GenBank under the accession QRAK00000000. The version described in this paper is version QRAK01000000.

The mass spectrometry proteomics data have been deposited to the ProteomeXchange Consortium via the PRIDE partner repository with the dataset identifier PXD010607.

GenBank accession numbers: Dehydrochlorinase (DHC_{M7}), MH703800; Haloalkane dehalogenase (HAD_{M7}), MH703801; Alcohol dehydrogenase (ADH_{M7}), MH703802; Mycothiol s-transferase, MH703803; Ring-cleaving dioxygenase, MH703804; *cis,-trans*-4-hydroxymuconic semialdehyde dehydrogenase, MH703805; Non-heme chloroperoxidase, MH703806; Mycothiol S-conjugate amidase, MH703807.

3. Results

3.1. Lindane influence upon Streptomyces sp. M7 growth

Sampling points for proteomics and transcriptional analyses were establish according to the growth of *Streptomyces* sp. M7 in MM_G and MM_L. Generation time in MM_G was 11 h and stationary phase of growth was reached after 24 h of incubation (Fig. S1). The presence of lindane affected the growth of *Streptomyces* sp. M7. Resembling an exponential phase of growth, a slight increase of the biomass was observed during the first 48 h of incubation (Fig. S1). Thus, for further analyses cells were harvested after 18 and 35 h of incubation in MM_G and MM_L respectively. These sampling points allowed obtaining comparable and metabolically active cells (exponential phase of growth). Lindane removal was 42% at the time that cells were harvested for proteomics and transcriptional studies.

3.2. Up-regulated proteins in the glucose and lindane proteomes were significant different

About 2050 different proteins were detected in *Streptomyces* sp. M7 protein extract (Table S2). It represents approximately 29% of the predicted protein sequences for this strain. 712 of these proteins, passed our significance parameters (see Material and Methods). 419 proteins in MM_G and 293 proteins in MM_L were identified as up-regulated (Fig. 1a). Analysis with the software BlastKoala (Kanehisa et al., 2016), showed that up-regulated proteins were distributed in metabolic pathways that result essential for a correct cellular operation (Fig. 1b). In MM_L we observed a slightly higher number of proteins involved in lipid metabolism and metabolism of molecules such as taurine, hypotaurine, β-Alanine and cyanoamino acids (Fig. 1b, category: metabolism of other amino acids). As expected, the number of proteins involved in "Xenobiotics biodegradation and metabolism" was higher in MM_L (Fig. 1b).

3.3. Central carbon metabolism and degrading pathways were active during lindane degradation in Streptomyces sp. M7

Enzymes from Embden-Meyerhof pathway were identified and some of them were up-regulated either in MM_G or MM_L. Interestingly, enzymes from pentose phosphate pathway including 6-phosphogluconolactonase, ribose 5-phosphate isomerase and ribokinase increased >2-fold their abundance in MM_L (Table 1). Transketolase and transaldolase enzymes from this pathway were
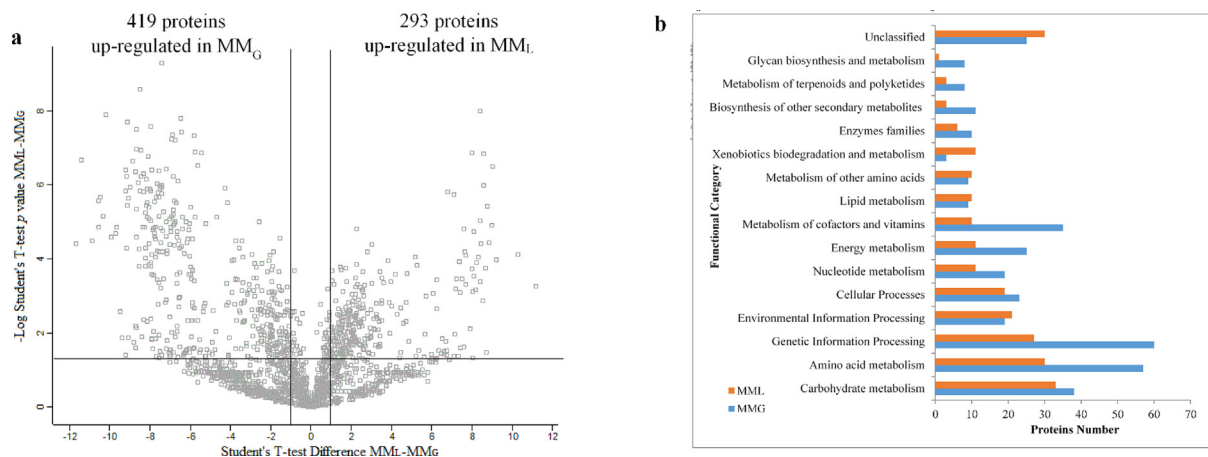
Fig. 1. **(a)** Protein dispersion plot. Proteome analyzed by the software Perseus showed a correct distribution of the identified proteins. **(b)** Functional categorization of up-regulated proteins in minimal medium supplemented with glucose (MMG) and lindane (MML).

also identified but they were slightly up-regulated in MM_L (approx. 1.5-fold) (Table S2). Regarding to tricarboxylic acid cycle enzymes, no significant difference in their abundances in MM_G and MM_L were detected. Likewise, enzymes comprising the electron-transfer chain and ATP synthase components showed similar abundance in both conditions (Table S2). Although they did not pass our significance level, glycogen-degrading enzymes such as glycogen debranching, phosphoglucomutase and glycogen phosphorylase were slightly up-regulated in MM_L (Table S2). Interestingly, this might suggest that glycogen degradation serves to feed pentose phosphate pathway. Enzymes involved in the degradation of fatty acids and metabolism of amino acids were also up-regulated in MM_L (Table 1). Amino acids metabolism was mostly related to catabolic reactions. Thus, enzymes such as valine dehydrogenase, betaine-aldehyde dehydrogenase and glycine cleavage system among others, which produce NADH/NADPH were up-regulated (Table 1).

3.4. Dechlorination and dehydrogenation reactions occur in the up-stream degradation pathway of lindane

LinA (dehydrochlorinase), LinB (haloalkane dehalogenase) and LinC (short chain alcohol dehydrogenase), compose the up-stream degradation pathway (Nagata et al., 1999). In MM_L, these enzymes were identified with a fold change higher than 2 (Table 1). The homotetrameric protein LinA is considered a unique type of dehydrogenase. This kind of dehydrogenase has no close relatives although they can present low sequence similarity to proteins with diverse functions (Nagata et al., 2001). The up-regulated dehydrochlorinase (DHC_{M7}) (MH703800) (379-fold) detected in *Streptomyces* sp. M7 showed 31% of similarity with LinA from *Sphingobium japonicum* UT26. In addition, the catalytic dyad D24 and H72 characteristic of LinA was present in DHC_{M7} (Fig. S2a) (Lal et al., 2010; Nagata et al., 2007). Regarding to microbial haloalkane dehalogenases and particularly LinB several variants for these enzymes were reported (Damborský and Koca, 1999; Lal et al., 2010; Streltsov et al., 2003). The *Streptomyces* sp. M7 haloalkane dehalogenase (HAD_{M7}) (MH703801) increased 10.5-fold its abundance in MM_L (Table 1). Instead of the high variability degree among LinB enzymes, HAD_{M7} showed 36% similarity with LinB from *S. japonicum* UT26. Based on the alignment and three-dimensional homology model discussed below, the residues D134, E239 and H265 would form the catalytic triad in HAD_{M7} (Fig. S2b). In contrast to LinA and B, few studies were addressed to the third up-stream

pathway enzyme. LinC belongs to the short chain alcohol dehydrogenase family (Nagata et al., 1994). In *Streptomyces* sp. M7 we identified an alcohol dehydrogenase (ADH_{M7}) (MH703802) that increased 2.9-fold its abundance in MM_L (Table 1). ADH_{M7} showed 52% of similarity with LinC from *S. japonicum* UT26. In addition, the catalytic triad Ser-Tyr-Lys and the conserved cofactor-binding motif (NAD^+) were identified (Fig. S2c). Up-stream degradation steps are resumed in Fig. 2.

3.5. Genes encoding DHC_{M7} (LinA), HAD_{M7} (LinB) and ADH_{M7} (LinC) were up-regulated by lindane

To asses our proteomic results and if the *in vivo* expression of DHC_{M7}, HAD_{M7} and ADH_{M7} is responsive to lindane, we compared the expression levels of these genes in MM_L and MM_G. The addition of lindane increased the expression levels of DHC_{M7}-2.8 folds, HAD_{M7}-10.9 folds and ADH_{M7}-2.5 folds (Fig. 3). Expression levels of these genes are in accordance with the higher abundance of their proteins in MM_L. These results suggest that expression of DHC_{M7}, HAD_{M7} and ADH_{M7} is specifically up-regulated by the addition of lindane.

3.6. Homology model for enzymes of the up-stream degradation pathway of lindane

Three-dimensional models of DHC_{M7} (LinA), HAD_{M7} (LinB) and ADH_{M7} (LinC) were constructed in order to identify active and binding sites. Fifty models were generated and evaluated for each protein. The best model was selected based on their DOPE score (Discrete Optimized Protein Energy). Distribution of φ and ψ torsion angles in the homology models and template structures are shown in Figures S3, S4 and S5. Overall, structural models for DHC_{M7}, HAD_{M7} and ADH_{M7} presented favorable stereochemistry (See supplementary material for a comprehensive explanation).

3.7. Enzymes of the down-stream degradation pathway of lindane were up-regulated

Few is currently known about enzymes that specifically participate in the called "down degradation of lindane". The up-stream described above and the down-stream pathways were proposed for the genus *Sphingobium* (Nagata et al., 1999). In actinobacteria and particularly in the genus *Streptomyces*, a complete degradation pathway was not proposed yet. The product of LinC, 2,5-

Table 1
Summary of up-regulated proteins of Streptomyces sp. M7 in the presence of lindane.

Protein Name; KO Number[a]	Function[b]	t-test (-log p Value)[c]	Average normalized area[d]		Fold Change[e]
Carbohydrate Metabolism			MM_L	MM_G	
Triosephosphate isomerase; K01803	Glycolysis	2.09	34.49	33.45	2.06
Phosphoglycerate mutase; K15634	Glycolysis	3.23	29.08	26.84	4.71
Pyruvate dehydrogenase E2 component; K00627	Glycolysis	2.63	28.76	25.77	7.95
Aldose 1-epimerase; K01785	Glucose Interconvertion (Glycolysis)	1.46	29.77	28.23	2.91
Phosphoenolpyruvate carboxykinase; K01596	Glycolysis	2.81	30.94	27.06	14.71
6-phospho-beta-glucosidase; K01222	Glycolysis	2.81	27.70	24.20	11.35
6-phosphogluconolactonase; K01057	Pentose phosphate pathway	2.26	30.30	28.14	4.48
ribose 5-phosphate isomerase; BK01808	Pentose phosphate pathway	3.48	32.06	29.84	4.65
Ribokinase; K00852	Pentose phosphate pathway	2.49	29.97	28.10	3.65
Phosphomannomutase; K01840	Fructose and mannose metabolism	1.37	29.69	28.14	2.92
L-fuculose-phosphate aldolase; K01628	Fructose and mannose metabolism	1.94	28.89	26.79	4.30
Beta-glucosidase; K05349	Starch and sucrose metabolism	2.11	27.46	24.35	8.68
Malto-oligosyltrehalose trehalohydrolase; K01236	Starch and sucrose metabolism	3.77	31.31	29.83	2.78
Beta-N-acetylhexosaminidase; K01207	Amino sugar and nucleotide sugar metabolism	2.44	30.01	28.44	2.98
Glucosamine-6-phosphate deaminase; K02564	Amino sugar and nucleotide sugar metabolism	3.39	29.10	27.33	3.39
Piruvate orthophosphate dikinase; K01006	Pyruvate metabolism	2.14	29.81	27.92	3.72
Trihydroxycyclohexane-1,2-dione acylhydrolase; K03336	Inositol phosphate metabolism	3.67	27.79	25.22	5.95
5-deoxy-glucuronate isomerase; K03337	Inositol phosphate metabolism	3.46	26.42	19.20	148.73
L-glyceraldehyde 3-phosphate reductase; K19265	Carbohydrate metabolism	2.56	30.21	28.57	3.11
Energy Metabolism					
NADH-quinone oxidoreductase subunit C; K00332	Oxidative phosphorylation	1.77	29.44	27.18	4.79
NADH-quinone oxidoreductase subunit E; K00334	Oxidative phosphorylation	2.82	31.15	29.28	3.67
NADH-quinone oxidoreductase subunit G; K00336	Oxidative phosphorylation	4.39	33.46	30.43	8.18
F-type H + -transporting ATPase subunit delta; K02113	Oxidative phosphorylation	2.38	30.27	27.15	8.69
Aerobic carbon-monoxide dehydrogenase; K03518	Oxidation of CO to CO_2	1.83	26.98	20.47	91.06
Lipid Metabolism					
Acetyl-CoA/propionyl-CoA carboxylase; K00626	Fatty acid degradation	2.39	28.88	26.25	6.22
Long-chain acyl-CoA ligase; K01897	Fatty acid degradation	2.17	29.73	27.35	5.22
Enoyl-CoA hydratase; K01692	Fatty acid degradation	1.70	27.58	25.52	4.17
Acyl-CoA dehydrogenase; K00249	Fatty acid degradation	3.91	26.55	19.20	163.26
Hydroxymethylglutaryl-CoA lyase; K01640	Degradation of ketone bodies	2.72	29.80	25.78	16.23
Dihydroxyacetone kinase; K05878	Glycerolipid degradation	1.80	31.95	30.85	2.14
Phosphatidylserine decarboxylase; K01613	Glycerophospholipid metabolism	1.42	30.01	28.90	2.15
Nucleotide Metabolism					
Phosphoribosylformylglycinamidine synthase; K01952	Purine metabolism	2.16	30.50	29.48	2.03
AICAR transformylase/IMP cyclohydrolase; K00602	Purine metabolism	2.24	32.75	31.36	2.61
5′-nucleotidase; K01081	Purine/pyrimidine metabolism	3.82	24.47	19.20	38.52
Nucleoside-diphosphate kinase; K00940	Purine/pyrimidine metabolism	1.67	32.68	31.66	2.03
XTP/dITP diphosphohydrolase; K02428	Purine metabolism	1.99	29.60	25.69	15.04
Adenylate kinase; K00939	Purine metabolism	1.48	31.77	30.50	2.41
5-hydroxyisourate hydrolase; K07127	Purine metabolism	3.44	25.47	19.20	77.05
Beta-ureidopropionase; K06016	Pyrimidine metabolism	2.74	26.66	24.56	4.28
Thymidine phosphorylase; K00758	Pyrimidine metabolism	4.81	31.00	28.72	4.85
NagD protein; K02566	Nucleotide transport and metabolism	1.44	30.10	29.04	2.09
Amino acid Metabolism					
4-aminobutyrate aminotransferase; K07250	Ala, Asp and Glu metabolism	1.79	32.61	30.40	4.63
1-pyrroline-5-carboxylate dehydrogenase; K00294	Ala, Asp and Glu metabolism	2.08	34.99	31.66	10.08
Glycine C-acetyltransferase; K00639	Gly, Ser and Thr metabolism	3.39	30.56	26.61	15.47
Primary-amine oxidase; K00276	Gly, Ser and Thr metabolism	2.52	28.48	25.69	6.91
Glycine dehydrogenase; K00281	Gly, Ser and Thr metabolism	1.47	31.05	29.50	2.94
Glycine cleavage system H protein; K02437	Gly, Ser and Thr metabolism	1.88	29.64	27.48	4.49
Betaine-aldehyde dehydrogenase; K00130	Gly, Ser and Thr metabolism	2.10	28.66	20.76	239.25
3-mercaptopyruvate sulfurtransferase; K01011	Cys and Met metabolism	1.65	30.88	29.04	3.60
Methionine-gamma-lyase; K01761	Cys and Met metabolism	4.45	28.06	19.20	464.79
Sulfur-carrier protein carboxypeptidase; K21140	Cys and Met metabolism	1.88	29.79	28.48	2.48
Valine dehydrogenase (NADP+); K00271	Val, Leu and Ile degradation	1.92	31.79	30.24	2.94
Methylmalonyl-CoA mutase; K01849	Val, Leu and Ile degradation	2.80	29.63	26.39	9.46
3-methylcrotonyl-CoA carboxylase beta subunit; K01969	Val, Leu and Ile degradation	2.49	29.80	25.52	19.46
Agmatinase; K01480	Arg and Pro metabolism	1.72	30.80	28.86	3.83
Ornithine–oxo-acid transaminase; K00819	Arg and Pro metabolism	2.67	30.37	27.74	6.18
Imidazoleglycerol-phosphate dehydratase; K01693	His metabolism	3.11	31.30	29.72	2.99
Imidazolonepropionase; K01468	His metabolism	1.96	27.90	20.77	140.49
4-hydroxyphenylpyruvate dioxygenase; K00457	Tyr and Phe metabolism	2.34	30.40	26.87	11.57
3-dehydroquinate dehydratase II; K03786	Phe, Tyr and Trp biosynthesis	2.68	28.74	26.20	5.83
Aspartate 1-decarboxylase; K01579	beta-Alanine metabolism	2.32	29.80	27.34	5.52
Pantoate–beta-alanine ligase; K01918	beta-Alanine metabolism	2.04	28.51	26.90	3.07
Gamma-glutamyltranspeptidase; K00681	Taurine metabolism	4.81	26.78	19.20	191.12
Xenobiotics biodegradation					
Dehydrochlorinase (DHC)	Up-stream HCH degradation	5.98	27.77	19.20	379.73
Haloalkane dehalogenase (HLD)	Up-stream HCH degradation	2.30	27.71	24.31	10.57

Table 1 (*continued*)

Protein Name; KO Number[a]	Function[b]	t-test (-log p Value) [c]	Average normalized area[d]		Fold Change[e]
Short chain alcohol dehydrogenase (ADH)	Up-stream HCH degradation	1.75	31.26	29.71	2.91
Mycothiol S-transferase (reductive dechlorinase)	Down-stream HCH degradation	1.43	27.91	21.30	97.47
Ring-cleaving dioxygenases	Down-stream HCH degradation	1.32	25.16	20.74	21.43
cis,trans-4-Hydroximuconic semialdehyde dehydrogenase	Down-stream HCH degradation	3.30	29.18	28.05	2.19
Mycothiol S-conjugate amidase; K18455	MSH-dependent detoxification	1.90	30.17	28.94	2.35
Non-heme chloroperoxidase; K00433	Chloride ions detoxification system	2.42	32.54	31.04	2.82
Acetyl-CoA acetyltransferase; K00626	Benzoate and ketonic bodies degradation	1.77	31.50	29.40	4.29
4-carboxymuconolactone decarboxylase; K01607	Benzoate degradation	6.84	27.80	19.20	386.99
2-aminobenzoate-CoA ligase; K08295	Aminobenzoate degradation	1.52	27.45	21.09	82.11
Homogentisate 1,2-dioxygenase; K00451	Styrene degradation	2.39	30.19	26.90	9.80
Fumarylacetoacetase; K01555	Styrene degradation	3.24	30.46	28.01	5.48
Transporters					
ATP-binding/permease protein; K21397	Membrane transport	2.09	30.68	27.47	9.21
ABC-substrate-binding protein; K02058	Membrane transport	1.32	29.65	28.50	2.22
ABC-ATP-binding protein; K02056	Membrane transport	3.34	27.24	24.22	8.14
ABC-substrate-binding protein; K02030	Membrane transport	3.08	25.27	19.20	67.21
ABC substrate-binding protein; K02030	Membrane transport	1.51	29.72	28.28	2.73
ABC ATP-binding protein; K02028	Membrane transport	2.61	26.28	24.69	3.02
ABC ATP-binding protein; K02003	Membrane transport	3.49	31.21	27.67	11.59
Ca-activated chloride channel homolog; K07114	Cl⁻ ion transporter	1.86	28.66	26.53	4.37
Osmoprotectant transport ATP-BP; K05847	ABC Transporters	1.44	27.64	24.77	7.35
BCAA transport permease protein; K01998	ABC Transporters	1.56	28.07	25.43	6.21
BCAA transport permease protein; K01999	ABC Transporters	1.56	28.31	26.78	2.90
PTS system; K02768	Phosphotransferase system (PTS)	3.16	29.10	26.55	5.86
Basic membrane protein A; K07335	Membrane porotein	3.77	31.45	29.71	3.35
Genetic Information Processing					
DNA-directed RNA polymerase; K03046	Transcription machinery	1.38	33.16	32.00	2.24
RNA polymerase sigma-70 factor; K03088	Transcription machinery	2.28	27.31	25.96	2.55
Transcription elongation factor GreA; K03624	Transcription machinery	1.78	30.62	28.36	4.80
Lrp/AsnC transcriptional regulator; K03719	Transcription factors	3.90	27.41	19.20	296.41
Lrp/AsnC transcriptional regulator; K03719	Transcription factors	2.24	31.94	30.20	3.33
Large subunit ribosomal protein L14; K02874	Translation/Ribosome	2.88	27.74	19.20	373.02
Large subunit ribosomal protein L20; K02874	Translation/Ribosome	4.91	28.16	19.20	497.64
Large subunit ribosomal protein L29; K02904	Translation/Ribosome	2.27	33.29	28.70	24.00
Aspartyl/Gln-tRNA amidotransferase; K02435	Aminoacyl-tRNA biosynthesis	1.91	29.28	25.84	10.87
Molecular chaperone DnaK; K04043	Messenger RNA biogenesis	1.50	32.15	30.57	2.99
Ribosome-binding factor A; K02834	Ribosome biogenesis	2.19	29.24	27.17	4.22
Ribosome maturation factor RimP; K09748	Ribosome biogenesis	3.73	27.21	19.20	258.58
Peptide chain release factor I; K02835	Translation factors	2.24	28.53	26.59	3.85
Ribosome recycling factor; K02838	Translation factors	2.49	32.02	29.81	4.62
DNA polymerase III subunit epsilon; K02342	DNA replication	3.99	28.40	19.20	589.61
DNA-3-methyladenine glycosylase I; K01246	DNA repair/replication	1.47	27.42	25.73	3.21
Uracil-DNA glycosylase; K03648	DNA repair/replication	1.44	29.76	28.53	2.35
Exodeoxyribonuclease III; K01142 E3.1.11.2	DNA repair/replication	2.16	29.17	27.76	2.64
Preprotein translocase subunit YajC; K03210	Protein export	2.60	30.59	28.71	3.67
Signal peptidase I; K03100	Protein export	1.48	28.46	26.98	2.80
Peptide-methionine (S)-S-oxide reductase; K07304	Protein folding and associated processing	1.69	30.58	28.98	3.03
DNase family protein; K03424	Replication proteins	2.25	29.24	26.81	5.40

[a] KEGG Orthology number assigned through BlastKoala search BRITE.

[b] According to KEGG pathways database.

[c] p-value were calculated as -log using Perseus software. Values over 1.3 means statistical significant difference between abundance in MM_L and MM_G.

[d] Average normalized area was calculated using three independent biological replicates. Values are represented as $\log_2$.

[e] Fold change was calculated using average normalized area values.

dichlorohydroquinone (2,5-DCHQ), may suffer a twofold reductive dechlorination mediated by LinD to yield chlorohydroquinone (CHQ) and hydroquinone (HQ) (Wells and Ragauskas, 2012). LinD is a type of glutathione S-transferase (GST) (Miyauchi et al., 1998). In MM_L, Streptomyces sp. M7 increased 97.4-fold the abundance of a sort of GST (Table 1). Instead of glutathione, members of the genus Streptomyces synthesize mycothiol (MSH) (Newton et al., 2011). MSH is the major antioxidant molecule in actinobacteria. Enzymes such as mycothiol S-transferase and mycothiol reductases are associated to its antioxidant activity. Thus, the probable LinD of Streptomyces sp. M7 would be rather a mycothiol S-transferase (MST) (MH703803). NADPH-dependent mycothiol reductases that reduce mycothione produced by MST were also identified in the proteome, although they did not pass our significant abundance parameters. In addition, a mycothiol S-conjugate amidase (MH703807) was up-regulated (2.3-fold) (Table 1). This enzyme is involved in the recycling of conjugated MSH produced by MST activity. The subsequent step, catalyzed by dioxygenases (LinE), comprises the cleavage of the HQ. Among the identified dioxygenases in our study, a ring-cleaving dioxygenase (MH703804) increased its abundance 21.4-fold in MM_L (Table 1). This enzyme presented the conserved domains typical of LinE enzymes (Miyauchi et al., 1999; Nagata et al., 1999). The product of LinE, the cis,trans-4-hydroxymuconic semialdehyde (HMSA), may be then converted to maleylacetate by a cis,trans-4-hydroxymuconic semialdehyde dehydrogenase. This enzyme (MH703805) was also detected with high abundance (2.1-fold) in MM_L (Table 1). Formation of maleylacetate suggests that subsequent degradation steps occur via β-ketoadipate pathway (β-KAP) to produce succinyl and acetyl-CoA. Although without significant differences between their
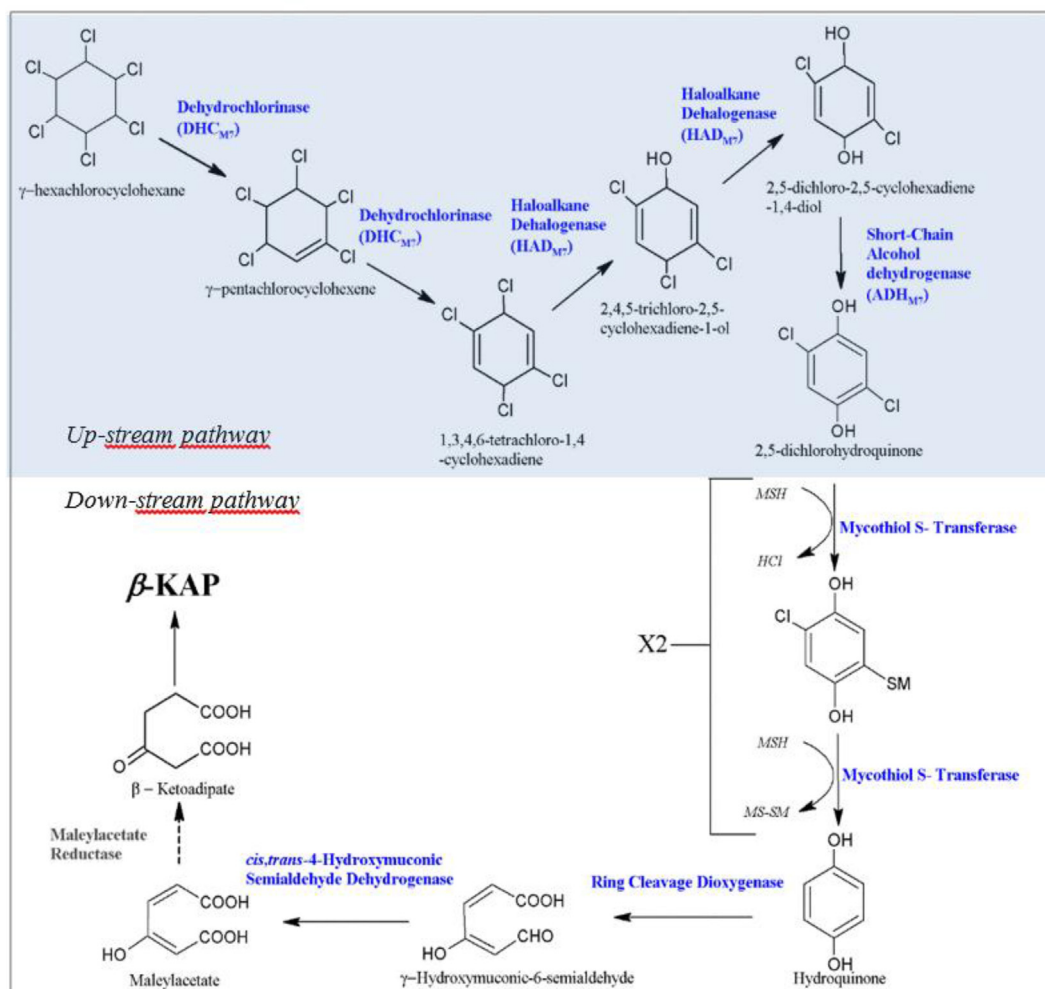
Fig. 2. Proposed degradation pathway for γ-hexachlorocyclohexane in *Streptomyces* sp. M7. Enzymes in blue were identified in the proteome and up-regulated in the presence of lindane. MSH: reduced mycothiol; MS-MS: Oxidized mycothiol (mycothione). MS-MS is reduced by mycothiol reductases regenerating thus mycothiol. (For interpretation of the references to colour in this figure legend, the reader is referred to the Web version of this article.)
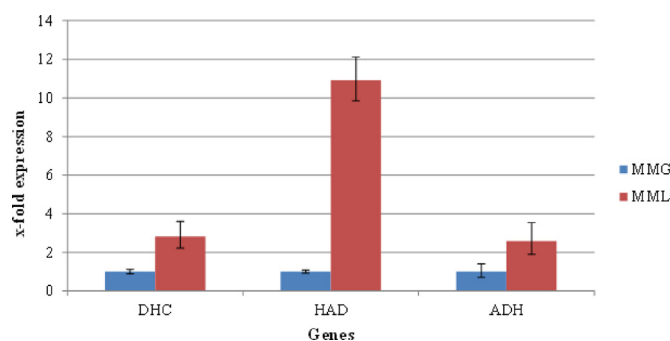

Fig. 3. Differential expression of up-stream degradation pathway enzymes. Dehydro-chlorinase (DHC); haloalkane dehalogenase (HAD); alcohol dehydrogenase (ADH). Minimal medium supplemented with glucose (MMG) and lindane (MML).

abundances in MM_L and MM_G, β-KAP enzymes were also identified (Table S1). The complete degradation is resumed in Fig. 2.

3.8. Chloride ions from dechlorination steps are eliminated by detoxification systems

Previous work reported the liberation of chlorine ions by

Streptomyces sp. M7 (Cuozzo et al., 2009; Sineli et al., 2016). Among several transporters, we identified a protein whose abundance increased 4.3-fold in MM_L (Table 1). BlastKOALA software classified this protein as Ca-activated chloride channel (*yfbK*). Chloride channels were studied in *Escherichia coli* and eukaryotic cells as chloride-proton antiporters (Chenal and Gunner, 2017; Matulef and Maduke, 2007). However, the mechanism of Ca-dependent chloride channel is unknown in bacteria able to degrade organochlorine compounds. These chloride channels might mediate the liberation of chloride ions outside the cell in *Streptomyces* sp. M7.

Another interesting finding in MM_L was the non-heme enzyme chloroperoxidase (MH703806). This enzyme catalyzes the production of HClO by moving one oxygen atom from H_2O_2 to Cl^-. Afterwards, it catalyzes the chlorination of aromatic or aliphatic compounds, through HClO, producing the corresponding chlorine species. Chloroperoxidase from *Streptomyces* sp. M7 was 2.8-fold up-regulated in MM_L (Table 1). Besides, it showed 83% identity with the well-characterized chloroperidase from *Streptomyces lividans* (Bantleon et al., 1994). Mechanisms, functionality and structure of chloroperoxidases were previously studied (Littlechild et al., 2002; Timmins and de Visser, 2015). Based on this background, this enzyme may serve as a detoxification tool for *Streptomyces* sp. M7 by eliminating H_2O_2 produced by the oxidative stress and Cl^- from dechlorination reactions.

4. Discussion

4.1. Metabolic context of lindane degradation

Streptomyces sp. M7 is one of the four strains of this genus reported as lindane degrader (Alvarez et al., 2017; Cuozzo et al., 2017; Lal et al., 2010). Works reported so far studied lindane degradation itself and the metabolic context was not considered. Global proteomic analysis revealed that pentose phosphate pathway was more active in the presence of lindane, probably at expenses of glycogen degradation. The up-regulation of key enzymes from pentose phosphate suggests a deviation of the carbon flux towards this pathway. Because of lindane recalcitrance and toxic intermediates formed during its degradation, we may assume that Streptomyces sp. M7 needs to activate its antioxidant mechanism. Pentose phosphate pathway is responsible for the supply of NADPH in cells. Thus, its activation in Streptomyces sp. M7 may be consequence of an increasing demand of NADPH required by several antioxidant enzymes. The actinobacteria Rhodococcus jostii RHA1 showed a similar behavior in the presence of the pro-oxidant methyl viologen (Dávila Costa et al., 2017). Catabolism of fatty acids and amino acids responded to the degradation of lindane. Thus, several enzymes that produce NADPH/NADH showed high abundance. Degradation of fatty acids and amino acids is expected upon adverse conditions. Undoubtedly, this metabolic context based on the generation of energy and reducing equivalents helps Streptomyces sp. M7 to offset the low level of energy obtained from lindane mineralization.

4.2. The up-stream degradation of lindane

Steps for the degradation of lindane in Streptomyces sp. M7 are proposed in Fig. 2. So far, the complete degradation pathway of lindane was only proposed in S. japonicum UT26 (Nagata et al., 2007). Crucial steps for the degradation are those from the up-stream pathway where four of the six chlorine atoms are eliminated. Mineralization of lindane is not possible without these initial steps. In this work, we identified the enzymes DHC_{M7}, HAD_{M7} and ADH_{M7} from the up-stream degradation pathway and demonstrated that they were up-regulated in the presence of lindane. Supporting our results, Cuozzo et al. (2009) determined dechlorinase activity and the product of DHC_{M7} in Streptomyces sp. M7. Unlike Streptomyces sp. M7, these enzymes were postulated as constitutive in S. japonicum UT26 although it was not proved by RT-qPCR (Nagata et al., 1999). Several variants of LinA, LinB and LinC were reported. Amino acid sequences of these enzymes significantly differ among bacterial genus (Lal et al., 2010). This may explain the low identity percentage obtained for DHC_{M7}, HAD_{M7} and ADH_{M7} alignments. In spite of this, three-dimensional homology models showed a proper folding of the proteins and a correct disposition of amino acids that form the active sites (S3, S4 and S5). Our results demonstrated that Streptomyces sp. M7 counts with the up-stream degradation pathway for lindane.

4.3. The down-stream degradation of lindane in Streptomyces sp. M7

The down-stream pathway is more complex than the up-stream in terms of number and variants of enzymes that can lead to the formation of TCA intermediates. Exist two possibilities for the degradation of 2,5-DCHQ. One of them, considered alternative pathway, consists of two reductive dechlorination and a ring cleavage mediated by LinD and LinE respectively, to form cis,trans-4-hydroxymuconic semialdehyde (Lal et al., 2010; Wells and Ragauskas, 2012). The reductive dechlorination is catalyzed by a glutathione S-transferase (GST) (Miyauchi et al., 1998). Since actinobacteria produce mycothiol instead of glutathione as antioxidant, it results illogical to assume that reductive dechlorination is catalyzed by a GST in these bacteria. In our study, the up-regulation of a mycothiol S-tranferase strongly suggests the participation of this enzyme in the reductive dechlorination of lindane. This hypothesis is supported by the identification and up-regulation of mycothiol-recycling enzymes (S-conjugate amidases and reductases) that can recycle the mycothiol used in this degradation step in Streptomyces sp. M7. Mycothiol-dependent enzymes and enzymes that recycle mycothiol are vital in the detoxification of xenobiotic agents (Newton et al., 2011; Rawat and Av-Gay, 2007). Regarding to ring cleavage, we identified five up-regulated dioxygenases. However only one of them counts with the conserved domains reported for LinE. Amino acid sequence of these enzymes widely differs according to the bacterial genus. Sphingobium japonicus UT26 encodes two LinE enzymes with 53% of identity (Endo et al., 2005). Not reliable LinE sequences were published for Streptomyces. Further studies will be conducted in order to elucidate if some of the dioxygenases encoded by Streptomyces sp. M7 corresponds to a new type of LinE. Lal et al. (2010) postulated as unknown the enzyme that catalyzes the conversion of cis,trans-4-hydroxymuconic semialdehyde to maleylacetate. Subsequently, Wells and Ragauskas (2012) proposed that this reaction is modulated by the cis,trans-4-hydroxymuconic semialdehyde dehydrogenase identified in Pseudomonas sp. WBC-3. Precisely, the up-regulation of a cis,trans-4-hydroxymuconic semialdehyde dehydrogenase in Streptomyces sp. M7 would lead to the formation of maleylacetate (Fig. 2; Table 1). Formation of maleyacetate ensures the complete degradation of lindane via the β-KAP (Wells and Ragauskas, 2012). β-KAP is present in a wide range of bacteria able to degrade hazardous pollutants. Often, other degradation pathways utilize the last two steps of β-KAP to complete the mineralization (Bala et al., 2010; Fairlee et al., 1997). Although we identified the last two enzymes of β-KAP in Streptomyces sp. M7, they did not show a fold change ˃2 in MM_L. This suggests that Streptomyces sp. M7 also uses these enzymes in MM_G or a fold change ˃2 is not necessary for a significant biological effect.

4.4. Transporters and liberation of chloride ions

The little is known about membrane transporters related to lindane degradation comes from Sphingobium. By random mutagenesis, Endo et al. (2007) identified an ABC-type transporter essential for the utilization of lindane in S. japonicum UT26. In addition, a comparative metagenomic analysis highlighted the abundance of ABC transporter genes in a lindane-degrading microbial community (Sangwan et al., 2012). These ABC transporters are related to the transport of lindane into the cell to facilitate the degradation (Dogra et al., 2004). Our proteomic analysis showed several components of ABC transporter with high abundance in MM_L (Table 1). Likewise Sphingobium, these ABC-type transporters might introduce lindane into Streptomyces sp. M7 thus facilitating its degradation.

Liberation of chloride ions outside the cell was previously demonstrated in Streptomyces sp. M7 (Cuozzo et al., 2009; Sineli et al., 2016). The unexpected finding of chloride channel in bacteria emerged from large-scale genome analyses (Iyer et al., 2002). Recently, Gururaja Rao et al. (2017) demonstrated the functionality of chloride channels in bacteria. The identification and up-regulation of a Ca-dependent chloride channel in Streptomyces sp. M7 opened a new research gate. To study the mechanism of these channels in bacteria that accumulate chloride ions by degradation of organochlorine molecules is our new challenge. In relation to the intracellular accumulation of chloride ions because of dechlorination reactions, interestingly we found an up-regulated

chloroperoxidase (Table 1). As described in results, this enzyme utilizes H_2O_2 and Cl^- as substrates. Chloroperoxidase and chloride channel might function together as chloride ions detoxification system in *Streptomyces* sp. M7.

5. Conclusion

The proteomic, transcriptional and bioinformatics analyses performed in *Streptomyces* sp. M7 allowed us to postulate a complete lindane-degrading pathway in actinobacteria for the first time. Lindane degradation is conducted through an up-stream and down-stream pathway. The enzymes that compose the up-stream pathway, indispensable for a success degradation, were identified and up-regulated in the presence of lindane. Enzymes from the down-stream pathway were also identified. The results indicated that part of the down-degradation occurs through an alternative pathway including (1) two reductive dechlorinations mediated by a mycothiol *S*-transferase; (2) cleavage of the hydroquinone mediated by a ring-cleaving dioxygenase; (3) formation of maleyacetate through a *cis,trans*-4-hydroxymuconic semialdehyde dehydrogenase.

Analysis of the metabolic context during lindane degradation indicated that pentose phosphate pathway and degradation of fatty acids and amino acids were turned on. NADPH produced in pentose phosphate pathway or degradation reactions would serve for the mycothiol reductases indirectly involved in the reductive dechlorination steps of the down-stream degradation pathway. Finally, the up-regulated ABC-type transporters would introduce lindane into the cell while chloroperoxidase and chloride channel would be involved in the homeostasis of chloride ions.

Declarations of interest

None.

Acknowledgements

Appendix A. Supplementary data

Supplementary data related to this article can be found at https://doi.org/10.1016/j.chemosphere.2018.08.035.

References

Alvarez, A., Saez, J.M., Davila Costa, J.S., Colin, V.L., Fuentes, M.S., Cuozzo, S.A., Benimeli, C.S., Polti, M.A., Amoroso, M.J., 2017. Actinobacteria: current research and perspectives for bioremediation of pesticides and heavy metals. Chemosphere 166, 41—62. https://doi.org/10.1016/j.chemosphere.2016.09.070.

Aparicio, J.D., Simón Solá, M.Z., Benimeli, C.S., Julia Amoroso, M., Polti, M.A., 2015. Versatility of *Streptomyces* sp. M7 to bioremediate soils co-contaminated with Cr(VI) and lindane. Ecotoxicol. Environ. Saf. 116, 34—39. https://doi.org/10.1016/j.ecoenv.2015.02.036.

Bala, K., Sharma, P., Lal, R., 2010. *Sphingobium quisquiliarum* sp. nov., a hexachlorocyclohexane (HCH)-degrading bacterium isolated from an HCH-contaminated soil. Int. J. Syst. Evol. Microbiol. 60, 429—433. https://doi.org/10.1099/ijs.0.010868-0.

Bantleon, R., Altenbuchner, J., van Pée, K.H., 1994. Chloroperoxidase from *Streptomyces lividans*: isolation and characterization of the enzyme and the corresponding gene. J. Bacteriol. 176, 2339—2347.

Benimeli, C.S., Amoroso, M.J., Chaile, A.P., Castro, G.R., 2003. Isolation of four aquatic streptomycetes strains capable of growth on organochlorine pesticides.

Bioresour. Technol. 89, 133—138. https://doi.org/10.1016/S0960-8524(03)00061-0.

Bindra, S., Scanlon, X.C., United Nations. Environment Programme, 2010. UNEP annual Report 2009 Seizing the Green Opportunity. United Nations Environment Programme (UNEP).

Chen, V.B., Arendall, W.B., Headd, J.J., Keedy, D.A., Immormino, R.M., Kapral, G.J., Murray, L.W., Richardson, J.S., Richardson, D.C., 2010. *MolProbity*: all-atom structure validation for macromolecular crystallography. Acta Crystallogr. Sect. D Biol. Crystallogr. 66, 12—21. https://doi.org/10.1107/S0907444909042073.

Chenal, C., Gunner, M.R., 2017. Two Cl ions and a glu compete for a helix cage in the CLC proton/Cl-antiporter. Biophys. J. 113, 1025—1036. https://doi.org/10.1016/j.bpj.2017.07.025.

Cuozzo, S.A., Rollán, G.G., Abate, C.M., Amoroso, M.J., 2009. Specific dechlorinase activity in lindane degradation by *streptomyces* sp. M7. World J. Microbiol. Biotechnol. 25, 1539—1546. https://doi.org/10.1007/s11274-009-0039-x.

Cuozzo, S.A., Sineli, P.E., Davila Costa, J., Tortella, G., 2017. *Streptomyces* sp. is a powerful biotechnological tool for the biodegradation of HCH isomers: biochemical and molecular basis. Crit. Rev. Biotechnol. 38 (5), 719—728. https://doi.org/10.1080/07388551.2017.1398133.

Damborský, J., Koca, J., 1999. Analysis of the reaction mechanism and substrate specificity of haloalkane dehalogenases by sequential and structural comparisons. Protein Eng. 12, 989—998. https://doi.org/10.1093/protein/12.11.989.

Dávila Costa, J.S., Herrero, O.M., Alvarez, H.M., Leichert, L., 2015. Label-free and redox proteomic analyses of the triacylglycerol-accumulating *Rhodococcus jostii* RHA1. Microbiology 161, 593—610. https://doi.org/10.1099/mic.0.000028.

Dávila Costa, J.S., Silva, R.A., Leichert, L., Alvarez, H.M., 2017. Proteome analysis reveals differential expression of proteins involved in triacylglycerol accumulation by *Rhodococcus jostii* RHA1 after addition of methyl viologen. Microbiology (United Kingdom) 163, 343—354. https://doi.org/10.1099/mic.0.000424.

Dogra, C., Raina, V., Pal, R., Suar, M., Lal, S., Gartemann, K.-H., Holliger, C., van der Meer, J.R., Lal, R., 2004. Organization of lin genes and IS6100 among different strains of hexachlorocyclohexane-degrading *Sphingomonas paucimobilis*: evidence for horizontal gene transfer. J. Bacteriol. 186, 2225—2235.

Endo, R., Kamakura, M., Miyauchi, K., Fukuda, M., Ohtsubo, Y., Tsuda, M., Nagata, Y., 2005. Identification and characterization of genes involved in the downstream degradation pathway of gamma-hexachlorocyclohexane in *Sphingomonas paucimobilis* UT26. J. Bacteriol. 187, 847—853. https://doi.org/10.1128/JB.187.3.847-853.2005.

Endo, R., Ohtsubo, Y., Tsuda, M., Nagata, Y., 2007. Identification and characterization of genes encoding a putative ABC-type transporter essential for utilization of γ-hexachlorocyclohaxane in *Sphingobium japonicum* UT26. J. Bacteriol. 189, 3712—3720. https://doi.org/10.1128/JB.01883-06.

Fairlee, J.R., Burback, B.L., Perry, J.J., 1997. Biodegradation of groundwater pollutants by a combined culture of *Mycobacterium vaccae* and a *Rhodococcus* sp. Can. J. Microbiol. 43, 841—846.

Goodfellow, M., 2012. Phylum XXVI. Actinobacteria phyl. nov. In: Bergey's Manual® of Systematic Bacteriology. Springer, New York, pp. 33—2028. https://doi.org/10.1007/978-0-387-68233-4_3.

Gururaja Rao, S., Ponnalagu, D., Sukur, S., Singh, H., Sanghvi, S., Mei, Y., Jin, D.J., Singh, H., 2017. Identification and characterization of a bacterial homolog of chloride intracellular channel (CLIC) protein. Sci. Rep. 7, 8500. https://doi.org/10.1038/s41598-017-08742-z.

Iyer, R., Iverson, T.M., Accardi, A., Miller, C., 2002. A biological role for prokaryotic ClC chloride channels. Nature 419, 715—718. https://doi.org/10.1038/nature01000.

Kanehisa, M., Sato, Y., Morishima, K., 2016. BlastKOALA and GhostKOALA: KEGG tools for functional characterization of genome and metagenome sequences. J. Mol. Biol. 428, 726—731. https://doi.org/10.1016/j.jmb.2015.11.006.

Lal, R., Pandey, G., Sharma, P., Kumari, K., Malhotra, S., Pandey, R., Raina, V., Kohler, H.-P.E., Holliger, C., Jackson, C., Oakeshott, J.G., 2010. Biochemistry of microbial degradation of hexachlorocyclohexane and prospects for bioremediation. Microbiol. Mol. Biol. Rev. 74, 58—80. https://doi.org/10.1128/MMBR.00029-09.

Littlechild, J., Garcia-Rodriguez, E., Dalby, A., Isupov, M., 2002. Structural and functional comparisons between vanadium haloperoxidase and acid phosphatase enzymes. J. Mol. Recogn. 15, 291—296. https://doi.org/10.1002/jmr.590.

Matulef, K., Maduke, M., 2007. The CLC "chloride channel" family: revelations from prokaryotes (Review). Mol. Membr. Biol. 24, 342—350. https://doi.org/10.1080/09687680701413874.

Miglioranza, K.S.B., Gonzalez, M., Ondarza, P.M., Shimabukuro, V.M., Isla, F.I., Fillmann, G., Aizpún, J.E., Moreno, V.J., 2013. Assessment of Argentinean Patagonia pollution: PBDEs, OCPs and PCBs in different matrices from the Río Negro basin. Sci. Total Environ. 452—453, 275—285. https://doi.org/10.1016/j.scitotenv.2013.02.055.

Miyauchi, K., Adachi, Y., Nagata, Y., Takagi, M., 1999. Cloning and sequencing of a novel meta-cleavage dioxygenase gene whose product is involved in degradation of gamma-hexachlorocyclohexane in *Sphingomonas paucimobilis*. J. Bacteriol. 181, 6712—6719.

Miyauchi, K., Suh, S., Nagata, Y., Takagi, M., 1998. Cloning and sequencing of a 2,5-dichlorohydroquinone reductive dehalogenase gene whose product is involved in degradation of y-hexachlorocyclohexane by *Sphingomonas paucimobilis*. J. Bacteriol. 180, 1354—1359.

Nagata, Y., Endo, R., Ito, M., Ohtsubo, Y., Tsuda, M., 2007. Aerobic degradation of lindane (γ-hexachlorocyclohexane) in bacteria and its biochemical and

molecular basis. Appl. Microbiol. Biotechnol. 76, 741–752. https://doi.org/10.1007/s00253-007-1066-x.

Nagata, Y., Miyauchi, K., Takagi, M., 1999. Complete analysis of genes and enzymes for γ-hexachlorocyclohexane degradation in *Sphingomonas paucimobilis* UT26. J. Ind. Microbiol. Biotechnol. 23, 380–390. https://doi.org/10.1038/sj.jim.2900736.

Nagata, Y., Mori, K., Takagi, M., Murzin, A.G., Damborský, J., 2001. Identification of protein fold and catalytic residues of gamma-hexachlorocyclohexane dehydrochlorinase LinA. Proteins 45, 471–477.

Nagata, Y., Ohtomo, R., Miyauchi, K., Fukuda, M., Yano, K., Takagi, M., 1994. Cloning and sequencing of a 2,5-dichloro-2,5-cyclohexadiene-1,4-diol dehydrogenase gene involved in the degradation of gamma-hexachlorocyclohexane in *Pseudomonas paucimobilis*. J. Bacteriol. 176, 3117–3125.

Newton, G.L., Leung, S.S., Wakabayashi, J.I., Rawat, M., Fahey, R.C., 2011. The DinB superfamily includes novel mycothiol, bacillithiol, and glutathione S-transferases. Biochemistry 50, 10751–10760. https://doi.org/10.1021/bi201460j.

Rawat, M., Av-Gay, Y., 2007. Mycothiol-dependent proteins in actinomycetes. FEMS Microbiol. Rev. 31, 278–292. https://doi.org/10.1111/j.1574-6976.2006.00062.x.

Sangwan, N., Lata, P., Dwivedi, V., Singh, A., Niharika, N., Kaur, J., Anand, S., Malhotra, J., Jindal, S., Nigam, A., Lal, D., Dua, A., Saxena, A., Garg, N., Verma, M., Kaur, J., Mukherjee, U., Gilbert, J.A., Dowd, S.E., Raman, R., Khurana, P., Khurana, J.P., Lal, R., 2012. Comparative metagenomic analysis of soil microbial communities across three hexachlorocyclohexane contamination levels. PLoS One 7, 1–12. https://doi.org/10.1371/journal.pone.0046219.

Simon Sola, M.Z., Pérez Visñuk, D., Benimeli, C.S., Polti, M.A., Alvarez, A., 2017. Cr(VI)

and lindane removal by *Streptomyces* M7 is improved by maize root exudates. J. Basic Microbiol. 57, 1037–1044. https://doi.org/10.1002/jobm.201700324.

Sineli, P.E., Tortella, G., Dávila Costa, J.S., Benimeli, C.S., Cuozzo, S.A., 2016. Evidence of α-, β- and γ-HCH mixture aerobic degradation by the native actinobacteria *Streptomyces* sp. M7. World J. Microbiol. Biotechnol. 32, 81. https://doi.org/10.1007/s11274-016-2037-0.

Streltsov, V.A., Prokop, Z., Damborský, J., Nagata, Y., Oakley, A., Wilce, M.C.J., 2003. Haloalkane dehalogenase LinB from *Sphingomonas paucimobilis* UT26: X-ray crystallographic studies of dehalogenation of brominated substrates. Biochemistry 42, 10104–10112. https://doi.org/10.1021/bi027280a.

Timmins, A., de Visser, S.P., 2015. Enzymatic halogenases and haloperoxidases: computational studies on mechanism and function. Adv. Protein Chem. Struct. Biol. 100, 113–151. https://doi.org/10.1016/bs.apcsb.2015.06.001.

Vijgen, J., Abhilash, P.C., Li, Y.F., Lal, R., Forter, M., Torres, J., Singh, N., Yunus, M., Tian, C., Schäffer, A., Weber, R., 2011. Hexachlorocyclohexane (HCH) as new Stockholm Convention POPs—a global perspective on the management of Lindane and its waste isomers. Environ. Sci. Pollut. Res. 18, 152–162. https://doi.org/10.1007/s11356-010-0417-9.

Wells, T., Ragauskas, A.J., 2012. Biotechnological opportunities with the β-ketoadipate pathway. Trends Biotechnol. 30, 627–637. https://doi.org/10.1016/j.tibtech.2012.09.008.

Wiederstein, M., Sippl, M.J., 2007. ProSA-web: interactive web service for the recognition of errors in three-dimensional structures of proteins. Nucleic Acids Res. 35, W407–W410. https://doi.org/10.1093/nar/gkm290.